Intra-marrow delivery of human interleukin-6-loaded biodegradable microspheres promotes growth of patient-derived multiple myeloma cells in mice

Multiple myeloma (MM) is an incurable malignancy of plasma cells in the bone marrow (BM). Historically, preclinical / translational MM research has largely relied on cell line-based models since patient-derived MM cells are well-known for being difficult to propagate *in vitro*,[1] and attempts to develop patient-derived xenograft (PDX) models based on subcutaneous, intravenous (i.v.) and orthotopic delivery of MM cells have had limited success. Genetic mouse models expressing human growth factors and cytokines have been developed to facilitate BM engraftment of human hematopoietic cells including MM cells, but those models failed to have a broad impact on the field, in part due to the limited access to models such as a human interleukin 6 (hIL-6) transgenic mouse model developed at Yale University in collaboration with Regeneron.[2] Several alternatives have been explored including injection of MM cells into the liver of neonatal immunodeficient mice,[3] subcutaneous implantation of rabbit bone grafts[4] or polymeric scaffolds[5] that were inoculated with patient-derived MM cells, or i.v. injection of unfractionated BM mononuclear cells from MM patients.[6] None of these methods have been widely adopted because of a variety of drawbacks. The former techniques are cumbersome and require a high degree of training, planning and co-ordination, and engraftment efficiency is highly variable; the latter approach lacks efficiency since it does not allow for serial engraftment of PDX-derived cells. Here we report the development of a MM PDX model via intra-marrow (IM) delivery of patient-derived MM cells (PDMMC) that were isolated from the pleural effusion of a patient with plasma cell leukemia (PCL), a rare and highly aggressive form of MM (*Online Supplementary Table S1*), and we show that co-injection of PDMMC with biodegradable porous polylactic-co-glycolic acid (PLGA) microspheres (MS) loaded with hIL-6 leads to enhanced expansion of PDMMC in immunodeficient mice (NOD/SCID/IL2Rg(null) [NSG]). The patient cells were collected under an institutional review board (IRB)-approved protocol after obtaining informed consent and following the relevant procedures according to the regulations established by the Clinical Research and Ethics Committee and the Helsinki Declaration of the World Medical Association. Our MS platform has the additional advantage that it can be utilized as a matrix to accommodate BM microenvironment-associated stromal cells such as osteoblasts[7] or endothelial cells[8] that are known for their ability to promote the survival of PDMMC. It can, therefore, be exploited both in the *in vitro* setting as a customizable three-dimensional (3D) co-culture system, and as an injectable adjuvant aiding MM PDX development. We fabricated porous PLGA MS with a diameter range of 100-200 μm using the double emulsion, i.e., water-in-oil-in-water (W/O/W) approach via a customized microfluidic device (Figure 1A). Decomposition of ammonium bicarbonate within the PLGA matrix at 34°C led to pore generation (Figure 1B, C). Upon further treatment with sodium hydroxide / ethanol solution to remove unwanted thin membranes between the pores, the pores became highly interconnected (Figure 1D, inset) with pore sizes ranging from 10 μm to 30 μm (Figure 1D), allowing various cell types, including anchorage-dependent stromal cells and MM cells, to be accomodated. To model the incorporation of bioactive factors for sustained release, bovine serum albumin (BSA) was loaded into MS either during the fabrication process (i.e., embedding) or via impregnation after MS fabrication. Compared to the high yet tunable amount (1 mg and 4 mg) of BSA that could be loaded in PLGA MS via the embedding approach, the amount that could be included via impregnation was relatively low (0.3 mg) (Figure 1E). Of note, surface-adsorbed BSA (impregnation) was released much faster than BSA embedded in the PLGA matrix, which primarily relies on diffusion and matrix degradation for release (Figure 1E, left). As a result, the 2 approaches of BSA incorporation led to different cumulative release profiles (Figure 1E, right), which could be exploited for dual delivery of payloads with distinct release kinetics. IL-6 has long been known as a crucial survival factor for MM cells.[9] We, therefore, fabricated hIL-6 loaded MS (hIL-6-MS) through the above-mentioned embedding approach and found that sustained release of hIL-6 from MS was achieved throughout the investigation period (11 days) despite an initial burst release (Figure 1F). More importantly, the released hIL-6 remained bioactive, and bioactivity closely correlated with the amount of hIL-6 initially loaded (Figure 1G), underscoring the potential of our platform to be employed as a molecularly tailored injectable adjuvant for humanization of the BM microenvironment of mice. Of note, degradation of our PLGA MS system *in vivo* (following IM injection) is expected to occur over a period of about four months.

Tumor necrosis factor-α (TNF-α) is another cytokine that has been implicated in MM cell growth and survival.[10] We, therefore, assessed PDMMC (CD138-selected PCL cells) maintenance *in vitro* comparing primary tumor cell (PTC) media (CloneExpress Inc., Gaithersburg, MD, USA) supplemented with hTNF-α, hIL-6, or both and found that the cocktail of both cytokines was superior to the other

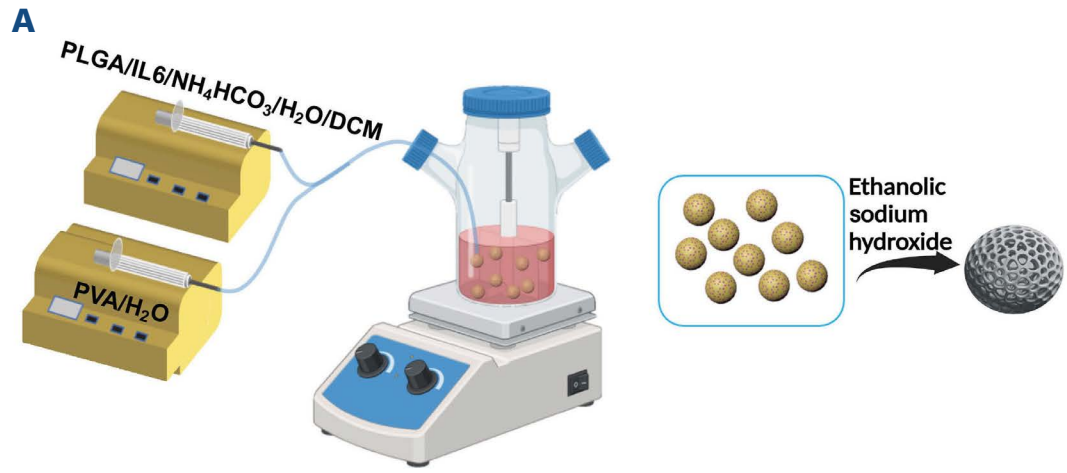

Figure 1. Porous polymeric microspheres can be used for local delivery of bioactive cytokines. (A) Schematic diagram of porous polylactic-co-glycolic acid (PLGA) porous microsphere (MS) fabrication via the water-in-oil-in-water (W/O/W) approach. (B) Stereomicroscopic image of as-prepared porous PLGA MS with backlighting. (C) Representative Scanning electron microscopy images of porous MS upon different post-fabrication treatments with sodium hydroxide / ethanol (left: 2-minute [min] treatment; right: 4-min treatment). (D) Average surface pore size of MS upon various post-fabrication treatments. (E) FITC-conjugated bovine serum albumin (BSA) was embedded or impregnated in PLGA MS. BSA-loaded MS were incubated in phosphate buffered saline (PBS) and BSA release was measured with a multimodal microplate reader using wavelength 560Ex/590Em. (Left) Release kinetics. (Right) Cumulative release. (F) Sustained release of recombinant human interleukin-6 (hIL-6) into 0.2 mL PBS from hIL-6-loaded MS (approx. 0.6 ng of hIL-6/sphere) as measured by enzyme linked immunosorbent assay (ELISA). (G) The bioactivity of released hIL-6 was determined via a bioluminescent cell-based hIL-6 bioassay. Error bars in the presented data show the standard error of the arithmetic mean (SEM). For non-survival pointwise analyses, non-parametric Mann-Whitney test was used for non-Gaussian distributions for comparison between 2 groups. $P<0.05$ was considered statistically significant. All statistical analyses were performed using GraphPad Prism 5 (La Jolla, CA, USA).

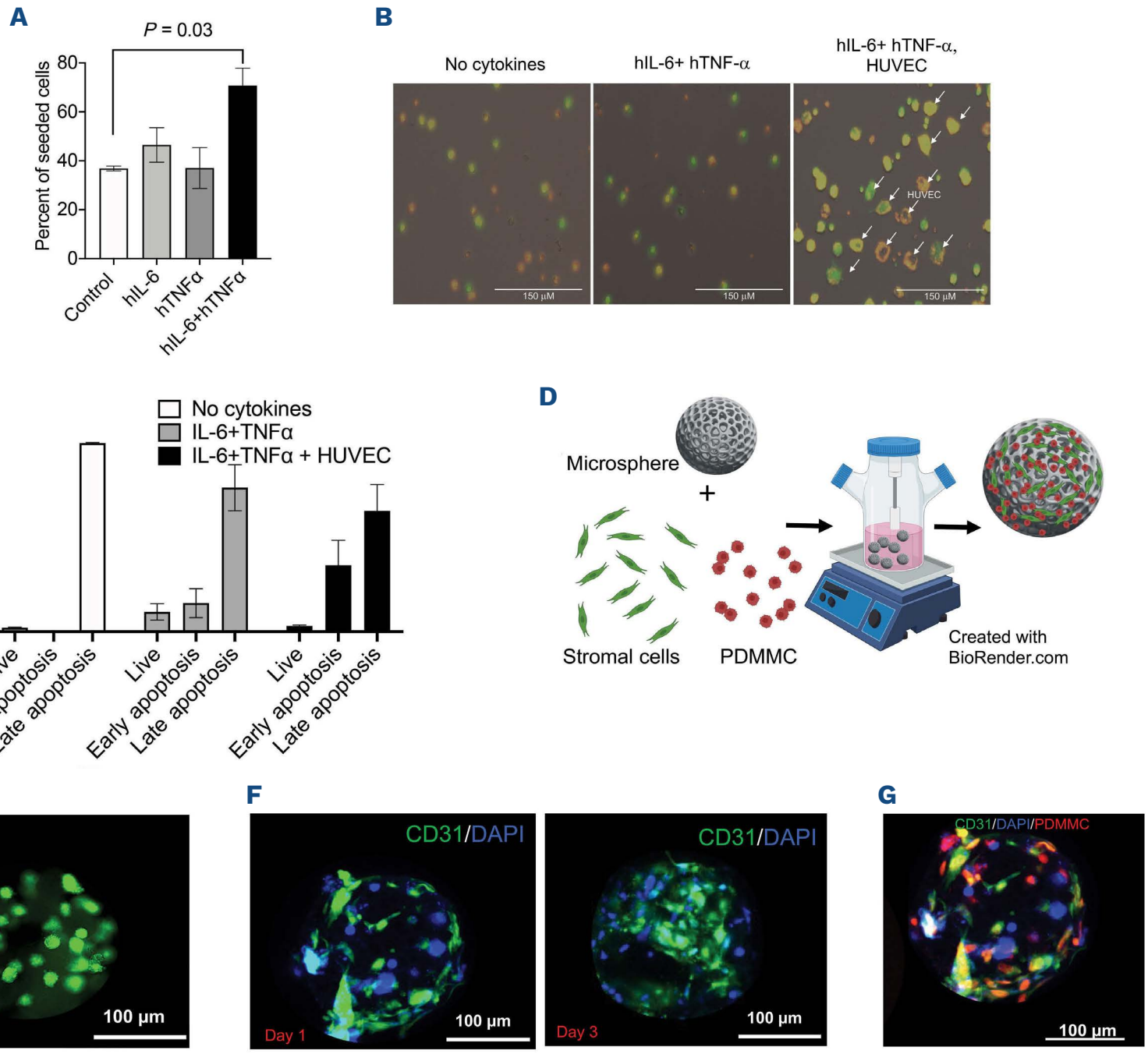

Figure 2. Patient-derived multiple myeloma cells *in vitro* viability is enhanced by media supplementation with human tumor necrosis factor-α and human interleukin-6, and by co-culture with endothelial cells. (A) Patient-derived multiple myeloma (MM) cells (PDMMC) were cultured in primary tumor cell (PTC) media with or without human tumor necrosis factor-α (hTNF-α), human interleukin-6 (hIL-6), or the cocktail of both cytokines. Mean and standard error of the arithmetic mean (SEM) of the percentage of seeded cells after 48 hours (hr) of culture are presented. (B and C) PDMMC were pre-labeled with PKH-26 and cultured in PTC media with or without hTNF-α + hIL-6 or hTNF-α + hIL-6+ endothelial cells (HUVEC). (B) Cells were stained with calcein AM and viability of PDMMC after 48 hr of culture was evaluated by live cell fluorescence microscopy. Dead cells: red/dark orange; live cells: yellow/green; arrows indicate HUVEC. (C) Cell viability (live: DAPI–Annexin V–; early apoptosis: DAPI–Annexin V+; late apoptosis: DAPI+) was assessed after 48 hr of culture by Annexin V assay. Mean and SEM are shown. (D) Schematic diagram depicting dynamic seeding and culture of endothelial cells and PDMMC onto polylactic-co-glycolic acid (PLGA) porous microspheres (MS). (E) Representative fluorescent images of HUVEC dynamically seeded and cultured on porous PLGA MS for 24 hr. Cells were stained for live (green) with calcein AM. (F) Representative confocal images of HUVEC-laden microspheres after culture for different periods (left: 24 hr; right: 72 hr). HUVEC were stained with FITC-conjugated anti-CD31 antibody and with DAPI for nuclei. (G) Representative confocal microscopy image of HUVEC-laden MS after co-culture for 24 hr with PKH-26-labeled PDMMC in PTC media supplemented with hTNF-α and hIL-6. HUVEC were stained with FITC-conjugated anti-CD31 antibody and with DAPI for nuclei. (H) Cell viability percentage of PDMMC co-cultured with HUVEC-laden MS *versus* cell-free MS in PTC media supplemented with hTNF-α and hIL-6. After 24 hr of culture, cells were stained with calcein AM and viability of PDMMC was evaluated by live cell fluorescence microscopy. Error bars in all presented data show the SEM. For non-survival pointwise analyses, non-parametric Mann-Whitney test was used for non-Gaussian distributions for comparison between 2 groups. $P<0.05$ was considered statistically significant. All statistical analyses were performed using GraphPad Prism 5 (La Jolla, CA, USA).

conditions (Figure 2A). Co-culture with human umbilical vein endothelial cells (HUVEC) further enhanced PDMMC viability (Figure 2B), slowing down, although not preventing, PDMMC apoptosis (Figure 2C). HUVEC have been reported to propagate PDMMC growth in 3D culture systems.[8] We utilized adenoviral protein E4-modified HUVEC in our study since E4 was shown to improve survival of primary endothelial cells.[11] We next used our MS platform as a matrix to accommodate PDMMC-supporting stromal cells such as osteoblasts or endothelial cells. While osteoblasts may promote myeloma cell dormancy,[12] robust evidence suggests that co-culture of PDMMC with human osteoblasts such as hFOB 1.19 cells promotes MM cell survival *in vitro*.[7,13] To achieve optimal cell seeding efficiency both on top of and

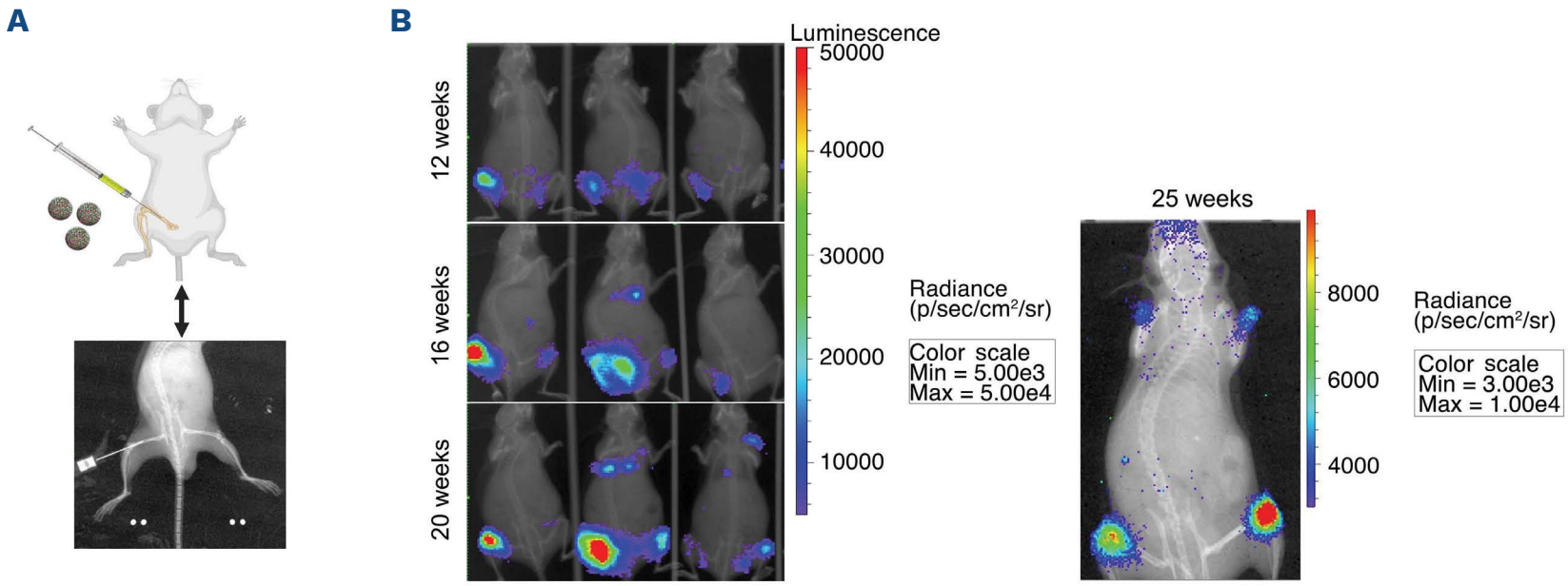

Continued on following page.

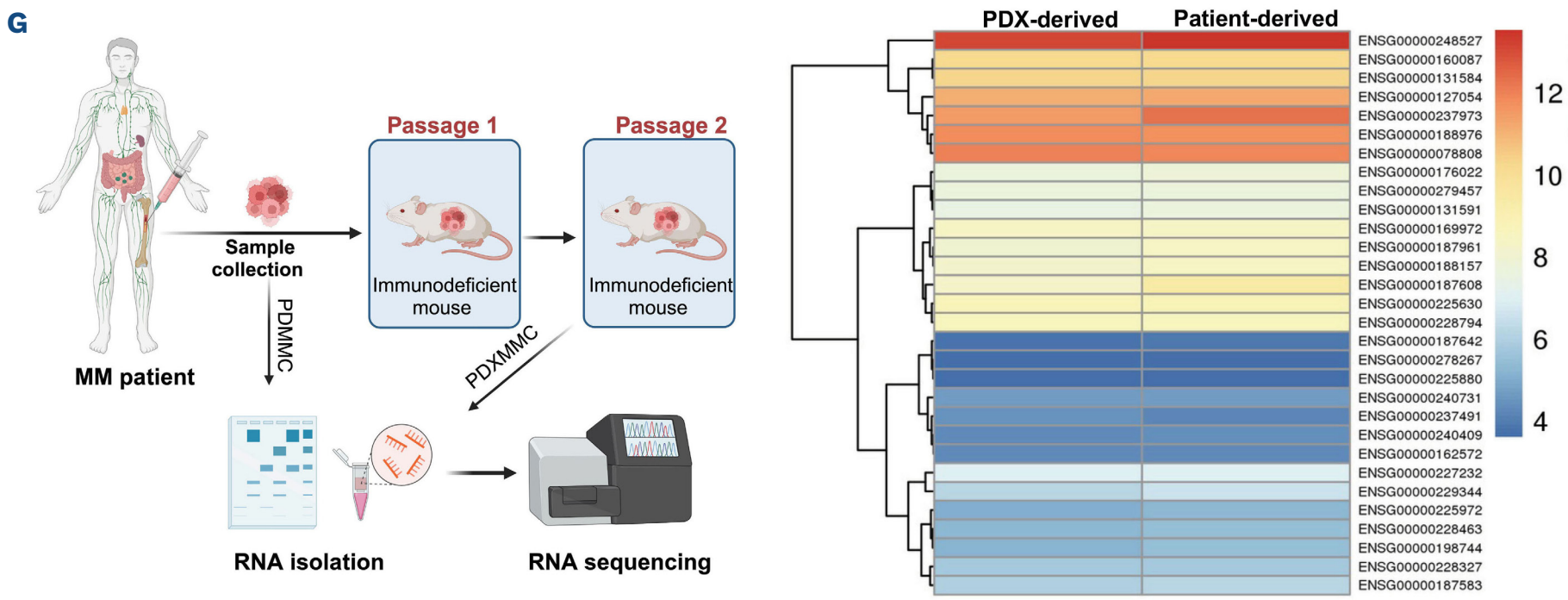

Figure 3. Intra-marrow co-injection of patient-derived multiple myeloma cells and human interleukin-6 establishes patient-derived multiple myeloma in NSG mice. (A) (Top) Schematic diagram of intra-marrow (IM) injection of an NSG mouse. (Bottom) X-ray shows the correct location of a needle in the medullary cavity of the right femur of an NSG mouse. (B) Firefly luciferase transduced patient-derived multiple myeloma (MM) cells (PDMMC) were delivered into the bone marrow (BM) of 4 NSG mice via bilateral intrafemoral injection. The tumor burden was monitored by *in vivo* bioluminescence (BLI) at 12, 16, and 20 weeks. Pseudocolor images superimposed on X-ray images of 3 mice are shown. A high-resolution X-ray/BLI image is shown for one mouse at 25 weeks. p/sec/cm^2/sr: photons per second leaving 1 cm^2 of tissue per steradian. (C-G) Sixteen NSG mice received an IM injection of 500,000 PDMMC and were divided into 4 groups: Control: PDMMC only; microspheres (MS)-human interleukin-6 (hIL-6): co-injection of PDMMC and MS-hIL-6; endothelial cells (HUVEC): co-injection of PDMMC and HUVEC; MS-hIL-6+ HUVEC: co-injection of PDMMC and HUVEC-laden and hIL-6 loaded MS. (C) H&E and CD138 immunohistochemistry (IHC) histological examinations of the BM were performed six months post injection. Images were acquired at 20x/40x magnification. Representative images of one mouse from each group are shown. Note: mouse megakaryocytes (indicated by asterisks) are negative for 3, 3'-diaminobenzidine (DAB) and surrounded by DAB+PDX-derived MM cell (PDXMMC). (D) BM mononuclear cells were analyzed for expression of human CD138 and human CD319 by multiparameter flow cytometry. Representative pseudocolor dot plots of one mouse from each group are shown. (E) BM mononuclear cells were analyzed for expression of human CD138, human CD319, and human κ light chain protein by multiparameter flow cytometry. (Left) Frequency of PDXMMC (based on CD139 and CD138 expression). (Middle) Median fluorescence intensity (MFI) of κ light chain expression by PDXMMC. (Right) MFI of CD138 expression by PDXMMC. Mean and standard error of the arithmetic mean (SEM) are shown. (F) Photographic images of extramedullary disease manifestations in 75% of the cases in 3 out of 4 mice in the MS-hIL-6 + HUVEC group six months post injection. (G) RNA-seqencing of the original PDMMC and PDXMMC from one of the tumor nodules shown in (F) after 2 passages through NSG mice. (Left) Schematic diagram of the workflow. (Right) Heatmap comparing the top 30 differentially expressed genes by adjusted *P* value using DESeq2. Error bars in all presented data show the standard error of the arithmetic mean (SEM). For non-survival pointwise analyses, non-parametric Mann-Whitney test was used for non-Gaussian distributions for comparison between 2 groups. $P<0.05$ was considered statistically significant. All statistical analyses were performed using GraphPad Prism 5 (La Jolla, CA, USA).

into porous MS, a spinner flask system was adopted for dynamic cell seeding and culture (Figure 2D). Both hFOB 1.19 cells and HUVEC adhered well to porous MS and remained viable while expanding for at least three days (Figure 2E, F, *Online Supplementary Figure S1*). Co-culture of PDMMC with HUVEC-laden MS revealed that PDMMC cells closely interacted with HUVEC (Figure 2G) and maintained good viability throughout the study period (Figure 2H). These experiments demonstrate that porous PLGA MS can be used as a matrix for stromal cells providing a favorable environment for MM cells, and they can be further modified for sustained release of MM survival-supporting biomolecules for PDX development.

To establish PDMMC growth in immunodeficient mice, PCL cells, hIL-6-MS, or a mixture of both were administered into the endosteal space via intrafemoral injection (Figure 3A). IM delivery of hIL-6-MS resulted in sustained *in vivo* release over a 15-day period, and importantly, this approach yielded a considerably higher concentration of hIL-6 in the mouse BM on day 8 after injection than IM delivery of free hIL-6 (*Online Supplementary Figure S2A*). Lentiviral transduction of frozen-thawed PCL cells with luciferase (pUltra-Chili-Luc; Addgene #48688) was shown to be feasible, enabling *in vivo* monitoring of the BM disease burden by bioluminescence imaging (Figure 3B). Of note, even though PDMMC are difficult to transduce (transduction efficiencies of 1-5%), a consistent bioluminescence signal can be obtained by accurate intrafemoral injection of a sufficient number (at least 10,000 cells, estimated) of luciferase-transduced cells. Serum free light chain ELISA is often used for *in vivo* monitoring of the disease burden in cell line-based MM mouse models, and we were able to detect low levels of free κ light chain protein in the serum of PDMMC recipients three months post injection (*Online Supplementary Figure*

S2B). *Ex vivo* (flow cytometric and histological) analysis of the BM six months post injection revealed a variable disease burden in all groups with a significantly increased frequency of PDMMC and upregulation of κ light chain protein in recipients of hIL-6-MS that were not seeded with HUVEC (Figure 3C-E). Surprisingly, co-injection of PDMMC with HUVEC-laden MS decreased the frequency of PDMMC in the BM, and CD138 levels of PDMMC were significantly decreased (Figure 3E), which may be due to heparanase activity from endothelial cells.[14,15] Furthermore, we found that extramedullary disease developed after 3-5 months in 50% of the cases when co-injecting hIL-6-MS and HUVEC (Figure 3F, *Online Supplementary Figure S2C*). While this unique formulation could be useful for *in vivo* expansion of PDMMC (i.e., for PDX-derived MM cell [PDXMMC] cell bank production), the preferred model for *in vivo* efficacy studies of novel MM drug candidates would be the establishment of robust BM disease by PDMMC/hIL-6 MS co-injection. Finally, we validated our model by transcriptome profiling of PDXMMC after 2 passages through immunodeficient mice, revealing that the PDXMMC genetically resembled the original PDMMC; expression levels showed no significant differences for the 2 compared datasets with a minimal adjusted *P*=0.999997 (Figure 3G).

In conclusion, we demonstrate the feasibility of MM PDX development-based IM injection of PCL cells combined with biomaterial-based hIL-6 delivery. It should be noted that the aggressiveness of PCL makes these cells uniquely exploitable for PDX model development, while the propagation of standard or low-risk MM cells in the BM of immunodeficient mice remains challenging even with hIL-6-MS co-injection (data not shown). Overall, the success of our innovative MS-based MM PDX model has the potential to advance translational MM research by enabling effective preclinical drug testing. This, in turn, may allow the development of novel therapeutics in this setting.

Authors

Manpreet Bariana,[1,2*] Weiwei Wang,[3,4*] Zhuozhuo Yin,[3] Jingyu Sun,[3] Shabnam Samimi,[1,5] Shaina A. Anuncio,[1] Elena Cassella,[1] Nuo Xu,[3] Wei Hu,[1] Ariel Aptekmann,[1] David S. Siegel,[1,6] Kar F. Chow,[7] Hongjun Wang[3,8#] and Johannes L. Zakrzewski[1,2,9,10#]

[1]Center for Discovery and Innovation, Hackensack Meridian Health, Nutley, NJ, USA; [2]Hackensack Meridian School of Medicine, Nutley, NJ, USA; [3]Department of Biomedical Engineering, Stevens Institute of Technology, Hoboken, NJ, USA; [4]School of Life Sciences, Yantai University, Yantai, Shandong, China; [5]Department of Chemistry and Chemical Biology, Stevens Institute of Technology, Hoboken, NJ, USA; [6]Multiple Myeloma Division, John Theurer Cancer Center, Hackensack University Medical Center, Hackensack, NJ, USA; [7]Department of Pathology, Hackensack University Medical Center, Hackensack, NJ, USA; [8]Semcer Center for Healthcare Innovation, Stevens Institute of Technology, Hoboken, NJ, USA; [9]Department of Oncology, Georgetown University, Washington, DC, USA and [10]Department of Pediatrics, Hackensack University Medical Center, Hackensack, NJ, USA

**MB and WW contributed equally as first authors.*
#HW and JLZ contributed equally as senior authors.

Correspondence:
H. WANG - hongjun.wang@stevens.edu
J. ZAKRZEWSKI - johannes.zakrzewski@hmh-cdi.org

https://doi.org/10.3324/haematol.2024.285980

Received: June 6, 2024.
Accepted: September 4, 2024.
Early view: September 12, 2024.

©2025 Ferrata Storti Foundation
Published under a CC BY-NC license

Disclosures

No conflicts of interest to disclose.

Contributions

MB, WW, ZY, JS, SS, SAA, EC, NX and WH are responsible for data curation. MB, WW, ZY, AA and JLZ are responsible for the formal analysis. MB, HW and JLZ validated the study. MB and KFC are responsible for study investigation. MB and AA are responsible for visualization. MB, WW, ZY, SAA, EC and KFC are responsible for methodology. MB and WW wrote the original draft. DSS, KFC, HW and JLZ are responsible for resources. DSS, HW and JLZ are responsible for project administration. HW and JLZ are responsible for the study concept, supervision, funding acquisition, and reviewing and editing the manuscript.

Acknowledgments

The authors would like to thank Dr. Jason Butler for kindly providing the HUVEC-E4 cells for this study, the Hackensack Meridian Health Biorepository for providing the MM patient cells, and the Flow Cytometry and the Microscopy & Imaging Core Facilities of the CDI.

Funding

JLZ received grant support from the National Cancer Institute (NCI 1R37CA250661-01A1), the Children's Leukemia Research Association, the American Society of Hematology, the International Myeloma Society, The New Jersey Health Foundation and the HMH Foundation/Tackle Kids Cancer. HW received grant support from the National Science Foundation (NSF-GCR award number 2219014).

Data-sharing statement

For original data, please contact johannes.zakrzewski@hmh-cdi.org. RNA-seq data are available at NCBI BioProject accession number PRJNA1146411.

References

1. Zlei M, Egert S, Wider D, Ihorst G, Wäsch R, Engelhardt M. Characterization of in vitro growth of multiple myeloma cells. Exp Hematol. 2007;35(10):1550-1561.
2. Das R, Strowig T, Verma R, et al. Microenvironment-dependent growth of preneoplastic and malignant plasma cells in humanized mice. Nat Med. 2016;22(11):1351-1357.
3. Crews LA, Balaian L, Delos Santos NP, et al. RNA splicing modulation selectively impairs leukemia stem cell maintenance in secondary human AML. Cell Stem Cell. 2016;19(5):599-612.
4. Yata K, Yaccoby S. The SCID-rab model: a novel in vivo system for primary human myeloma demonstrating growth of CD138-expressing malignant cells. Leukemia. 2004;18(11):1891-1897.
5. Calimeri T, Battista E, Conforti F, et al. A unique three-dimensional SCID-polymeric scaffold (SCID-synth-hu) model for in vivo expansion of human primary multiple myeloma cells. Leukemia. 2011;25(4):707-711.
6. Li C, Jethava Y, Frech I, Zhan F. Development of an easily accessible patient-derived xenograft (PDX) mouse model in multiple myeloma. Blood. 2019;134(Suppl 1):5538.
7. Zhang W, Gu Y, Sun Q, et al. Ex vivo maintenance of primary human multiple myeloma cells through the optimization of the osteoblastic niche. PLoS One. 2015;10(5):e0125995.
8. Belloni D, Heltai S, Ponzoni M, et al. Modeling multiple myeloma-bone marrow interactions and response to drugs in a 3D surrogate microenvironment. Haematologica. 2018;103(4):707-716.
9. Treon SP, Anderson KC. Interleukin-6 in multiple myeloma and related plasma cell dyscrasias. Curr Opin Hematol. 1998;5(1):42-48.
10. Jourdan M, Tarte K, Legouffe E, Brochier J, Rossi JF, Klein B. Tumor necrosis factor is a survival and proliferation factor for human myeloma cells. Eur Cytokine Netw. 1999;10(1):65-70.
11. Zhang F, Cheng J, Hackett NR, et al. Adenovirus E4 gene promotes selective endothelial cell survival and angiogenesis via activation of the vascular endothelial-cadherin/Akt signaling pathway. J Biol Chem. 2004;279(12):11760-11766.
12. Khoo WH, Ledergor G, Weiner A, et al. A niche-dependent myeloid transcriptome signature defines dormant myeloma cells. Blood. 2019;134(1):30-43.
13. Zhang W, Lee WY, Siegel DS, Tolias P, Zilberberg J. Patient-specific 3D microfluidic tissue model for multiple myeloma. Tissue Eng Part C Methods. 2014;20(8):663-670.
14. Jung O, Trapp-Stamborski V, Purushothaman A, et al. Heparanase-induced shedding of syndecan-1/CD138 in myeloma and endothelial cells activates VEGFR2 and an invasive phenotype: prevention by novel synstatins. Oncogenesis. 2016;5(2):e202.
15. Godder K, Vlodavsky I, Eldor A, Weksler BB, Haimovitz-Freidman A, Fuks Z. Heparanase activity in cultured endothelial cells. J Cell Physiol. 1991;148(2):274-280.